Farooqui and Saengudomlert *EURASIP Journal on Wireless Communications and Networking* 2013, **2013**:138
http://jwcn.eurasipjournals.com/content/2013/1/138

EURASIP Journal on Wireless Communications and Networking
a SpringerOpen Journal

RESEARCH Open Access

Transmit power reduction through subcarrier selection for MC-CDMA-based indoor optical wireless communications with IM/DD

Muhammad Zubair Farooqui* and Poompat Saengudomlert

Abstract

This research addresses the issue of average transmit optical power reduction in multi-carrier code division multiple access (MC-CDMA)-based indoor optical wireless communications employing intensity modulation with direct detection. The problem is treated in a novel way by investigating pre- and post-equalization-based subcarrier selection for transmit power reduction in downlink transmissions. Analytical expressions are derived for upper bounds of the required fixed DC bias for both cases. The fixed DC bias is used to reduce the system complexity on one hand and to devise optimal subcarrier selection criteria on the other. Simulation results based on the proposed subcarrier selection reveal significant power reduction subject to the 10^{-4} bit error rate (BER) requirement for 10-Mbps 64-subcarrier MC-CDMA-based indoor optical wireless communication systems. In addition, the BER performance obtained from pre-equalization is shown to be no higher than that obtained from post-equalization for the same transmit power.

1 Introduction

Multi-carrier and multiple access communication technologies like orthogonal frequency division multiple access (OFDMA) and multi-carrier code division multiple access (MC-CDMA) have captured different vistas of communications not only for simple text data but also for different types of multimedia requiring robust transmissions. For 4G wireless systems [1] and beyond, optical wireless communication is considered as a linchpin to serve as a complementary sibling of RF for system implementation in indoor environments. Although multi-carrier models, especially OFDM-based, have been much investigated, relatively few work can be observed regarding the use of MC-CDMA for indoor optical wireless communications.

Recently optical wireless systems are reported to be integrated with WiFi networks to provide ubiquitous coverage systems for indoor applications [2]. In these systems, the optical spectrum provides an encouraging potential as a complementary medium to the congested radio spectrum. For such applications, intensity modulation (IM) can be applied to either infrared or visible light. The key advantages of such optical wireless systems are usage of flexible unlicensed spectrum, high data rate support, energy efficiency, no electromagnetic interference, low-cost front ends, and inherent security. Major issues are eye and skin safety problems which can be dealt with by limiting the average transmit optical power.

The contributions of this research, which are not reported previously to the best of the authors' knowledge, are highlighted as follows:

1. Average transmit optical power reduction is accomplished by subcarrier selection for the first time in MC-CDMA-based indoor optical wireless communication systems employing intensity modulation with direct detection (IM/DD).
2. Expressions for upper bounds of a fixed DC bias using pre- and post-equalization-based subcarrier selection are analytically derived for MC-CDMA-based IM/DD system.
3. Optimal subcarrier selection algorithms that minimizes the bit error rate (BER) for a fixed transmit optical power are proposed for both pre- and post-equalization.

*Correspondence: zubair.research@gmail.com
Telecommunications Field of Study, School of Engineering and Technology, Asian Institute of Technology (AIT), Klong Luang, Pathumthani 12120, Thailand

This paper is organized as follows. In Section 2, relevant works are discussed. Section 3 presents the proposed system model. Results and discussions are given in Section 4. Finally, conclusions are given in Section 5.

2 Related works

2.1 Average transmit power issue in multi-carrier optical wireless communications

One major difference between an optical IM/DD channel and a conventional radio/electrical channel is that the channel input and output are signal intensities. This property has two major consequences - the input to the optical channel must be nonnegative, while the average transmit optical power is proportional to the mean (first moment contrary to second moment for electrical domain) of the input to the channel [3]. The former requires that an optical signal be unipolar, leading to the addition of a DC bias to the transmit signal. Despite the fact that the addition of symbol-by-symbol DC bias seems theoretically simple, it results in a significant increase in system implementation complexity. Hence, using a fixed DC bias is practically attractive. The use of a DC bias results in a high transmit power which may be hazardous for eye and skin safety [4,5]. Moreover, this additional power does not increase the SNR at the receiver at all [6]. Therefore, some appropriate power reduction scheme is required so that the associated DC bias does not lead to excessive transmit optical power [7].

The Infrared Data Association (IrDA), ANSI, and IEC standards recommend to limit the transmit optical power for different applications to address eye and skin safety problems at length [8,9]. Hence, being equivalent in connotation to the issue of peak-to-average power (PAPR) reduction in radio transmissions, transmit power reduction is at the crux of researches in multi-carrier optical wireless communications. While the issue has been investigated for OFDM-based optical wireless systems, to the best of the authors' knowledge, any direction of reparation of this issue has not yet been reported for MC-CDMA-based optical wireless systems with IM/DD.

For simple multi-carrier-based and OFDM-based indoor optical wireless communications, the following prominent solutions were put forth to address the issue of average power reduction. Block coding was investigated in [3] using symbol-by-symbol bias for power reduction. An approach based on optimized reserved subcarriers was investigated in [10] . Clipped OFDM was suggested in [7] instead of conventional DC bias for achieving power reduction. The technique is claimed to have better power efficiency when compared to the DC bias approach. According to [11], clipped OFDM attains some advantages over DC-biased OFDM but at the cost of sacrificing a reasonable chunk of the available signaling bandwidth. The authors of [12] addressed the same issue by employing in-band coding to use with symbol-by-symbol bias. A novel approach of using out-of-band subcarriers to reduce transmit power was proposed in [13]. The use of the selected mapping technique was investigated in [14] to achieve reduction in average transmit optical power. A simple power allocation approach was suggested in [15] to achieve power reduction for a specific BER requirement. In [16], sparsity together with uncertainty principle was used for average power reduction. The authors in [17] proposed the use of Hartley transform module instead of inverse fast Fourier transform (IFFT) module to assure real positive output, eliminating the need of adding DC bias and greatly enhancing the power efficiency in OFDM-based optical IM/DD systems. However, none of the works have been found reported for transmit power reduction in MC-CDMA with IM/DD.

2.2 Optical wireless channel

The key distinction between a conventional electrical channel and an IM/DD optical channel is that data are transmitted through the optical channel in the form of signal intensity. Accordingly, an IM/DD optical wireless system imposes the constraint that the transmitted signal should be real-valued and nonnegative to appropriately drive the light source [18]. Moreover, there is no multi-path fading due to a typically high ratio between a photodetector area and an optical wavelength [8].

From [8], the baseband model for an optical IM/DD channel in a diffused configuration can be mathematically represented as

$$Y(t) = RX(t) \otimes h(t) + N(t), \tag{1}$$

where

$$h(t) = H(0)\frac{6a^6}{(t+a)^7}u(t), \tag{2}$$

$Y(t)$ is the output photocurrent of the photodetector, R is the detector responsivity, and $\otimes$ is the convolution operation. The IM/DD optical channel impulse response $h(t)$ is dependent on the channel DC gain $H(0)$ and a factor a which further depends on the rms delay spread D such that $a = 12\sqrt{\frac{11}{13}}D$.

The prominent cause of noise is visible background light (fluorescent light, incandescent light, and sunlight), which is independent of the nature of the signal and modeled as additive white Gaussian noise (AWGN) [19], denoted by $N(t)$. Finally, $u(t)$ is the unit step Heaviside function.

2.3 MC-CDMA

Owing to its high spectral efficiency, flexibility, and endurance to frequency-selective fading, MC-CDMA, an amalgam of OFDM and CDMA based on the principle of frequency domain spreading, has emerged as a strong

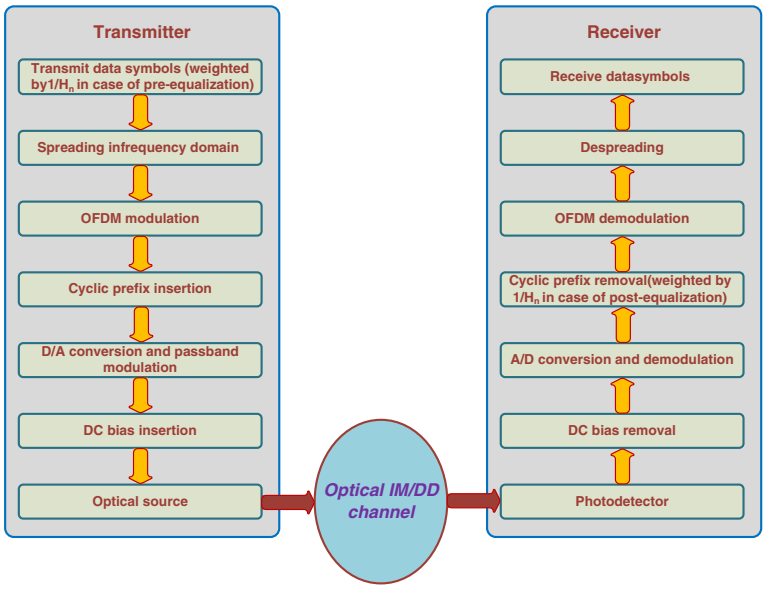

Figure 1 MC-CDMA-based indoor wireless optical system with IM/DD.

candidate for future communication systems in recent years. In the last decade, MC-CDMA has attracted lots of interests in the research community, especially for downlink applications, where frequency domain equalization techniques can be used to mitigate multi-access interference (MAI) that arises due to multi-path propagation. No significant linear distortion is confronted in MC-CDMA because the symbol duration is much longer than the delay spread. MC-CDMA also offers flexible system design since the length of orthogonal signatures distinguishing multiple users from one another need not be equal to the number of subcarriers [20].

The working of MC-CDMA is such that an individual user's complex-valued data symbol is spread over OFDM subcarriers in the frequency domain using a spreading code. These symbols from different users are summed in the frequency domain and then passed to the OFDM modulator to transform into the time domain. A cyclic prefix is appended to mitigate inter-symbol interference with the result upconverted to the passband after serial-to-parallel conversion. At the receiver side, cyclic prefix removal, FFT, and despreading are carried out respectively.

2.4 Equalization

Channel equalization is a crucial phase in wireless communication systems. Due to the frequency-selective nature of wireless communication channels, spread spectrum schemes suffer impairments in orthogonality, which can be restored using different equalization techniques. In essence, the exploitation of appropriate equalization helps to efficiently combine different subcarriers' signals in order to optimize the system performance [21]. Equalization requires the availability of channel estimates at the receiver or at the transmitter or at both ends depending upon the case of post-, pre- or combined equalization, respectively. Pre-equalization focuses on pre-compensating the predictable channel distortions. Conventionally, MAI mitigation in MC-CDMA systems is carried out by single-user or multi-user detection schemes (SUD or MUD) at the receiver [22]. Equalization

Table 1 Simulation parameters

Parameter	Specification
Transmission bit rate	10 Mbps
Modulation	QPSK
Number of subcarriers	64
Spreading sequences	Walsh-Hadamard
Channel model	As in (2) [8]
Equalization	Single-tap frequency domain pre- and post-equalization
Digital-to-analog converter (DAC)	Rectangular pulse
$H(0)$ (DC channel gain)	−60 dB [8]
N_0 (noise variance)	10^{-23} A^2/Hz [8]
D (rms delay spread)	10 ns [8]
R (photodetector responsivity)	1 A/W [8]
Transmit power calculation	As per multi-carrier optical wireless communications

is preferred over SUD and MUD techniques in terms of system complexity [23-25].

Equalization may be linear or nonlinear [26]. Equal gain combining, maximal ratio combining, orthogonality restoring combining, and minimum mean square error techniques are some versions of linear equalization employed in MC-CDMA, where appropriate coefficients are used as weighting factors for the signals from different subcarriers. Interference cancellation and maximum likelihood detection are examples of nonlinear equalization which provide performance improvement at a tradeoff with receiver complexity [27]. The authors in [28] demonstrated the significant dependence of PAPR on the equalization technique and exploited equalization coefficients for PAPR reduction in MC-CMDA systems.

3 Proposed system

3.1 Methodology

In this research, we demonstrate how subcarrier selection can be exploited to achieve reduction in average transmit optical power in MC-CDMA-based indoor optical wireless communications with IM/DD. We propose subcarrier selection based on linear equalization, which is considered to be the simplest and least expensive technique to be implemented [26] to mitigate various impairments in conventional MC-CDMA systems. Along with taking advantage of these positive features of linear equalization, we derive upper bounds for obtaining fixed DC bias values for both and pre- and post-equalization in MC-CDMA-based indoor optical wireless communications with IM/DD. Based on these upper bounds, we devise subcarrier selection criteria for both pre- and post-equalization implementation.The subcarrier selection algorithms obtained analytically are used in the simulation to observe the average transmit optical power reduction separately for both cases.

Optical wireless channels exhibit frequency-selective nature at high data rates for multi-carrier signals. To use the transmission bandwidth efficiently, subcarriers with better channel gains are used through an equalization-based criterion. For this, we investigate downlink optical wireless transmissions with the data rates of 10 Mbps, which is considered moderate for optical wireless-based industrial applications [1,2]. The mentioned data transmission rate is used, keeping in view the two important factors in considering IR-based indoor optical wireless systems with diffused configuration. Firstly, the standards framed by IrDA and IEEE for typical room sizes in indoor optical wireless systems are of the order of this range [9,29]. Secondly, the operating speed of currently available commercial devices in the market is typically in the same order as for our system. According to [30], there are theoretical limits and practical constraints like suitable optical sources and drive electronics in achieving high data rates for such systems. Data transmissions are simulated separately using MATLAB (MathWorks Inc., Natick, MA, USA), for pre- and post-equalization cases. The key parameters used for the selection of subcarriers are the channel gains of individual subcarriers. Since channel variations are slow in indoor environments, the channel state information (CSI) derived at a particular instant can be used for some subsequent time duration in indoor optical wireless systems. Subcarrier selection for MC-CDMA can be further advocated by the fact that different subcarriers contain information on the same data symbol; therefore, noise-dominated subcarriers can be discarded and signal energy can be reallocated to better subcarriers.

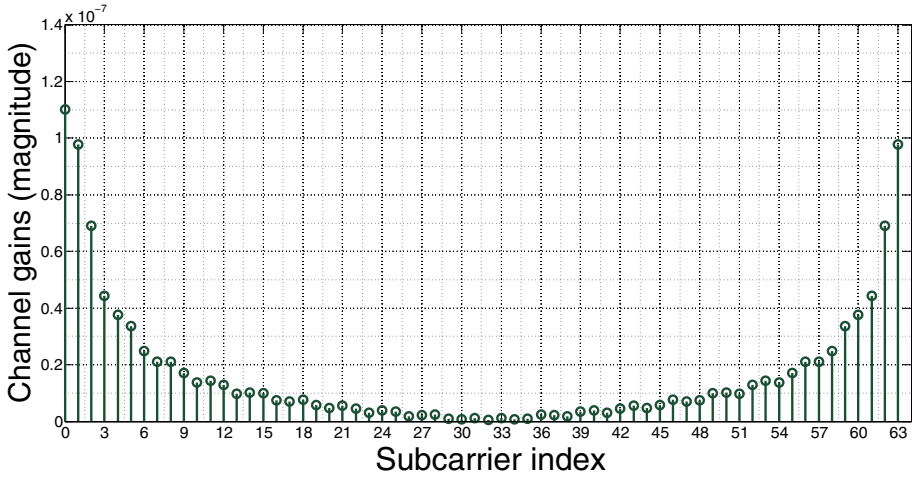

Figure 2 Channel gains for 64 subcarriers at 10 Mbps.

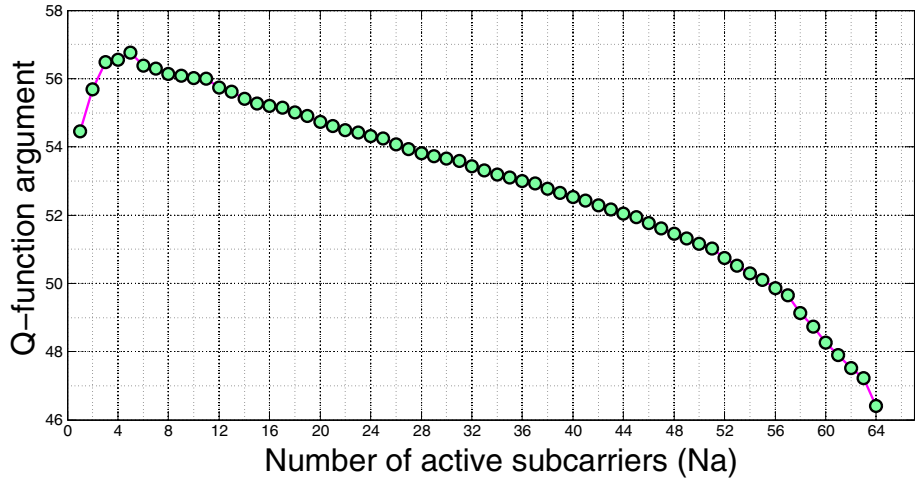

Figure 3 Q function argument vs. number of active subcarriers for the radio domain.

3.2 System model

The system model is specified by the following notations. For analysis, it is sufficient to focus on the transmission of a single symbol from each user:

- L, number of active users
- N, number of subcarriers
- $N_{\mathrm{cp}} = \gamma N$, length of cyclic prefix where $0 \leq \gamma \leq 1$
- $\mathcal{N}_{\mathrm{a}}$, set of active (selected) subcarrier indices
- N_{a}, number of active subcarriers indices, i.e., $N_{\mathrm{a}} = |\mathcal{N}_{\mathrm{a}}|$
- d_l, data symbol from user l
- $c_{l,n}$, CDMA codeword component for user l on subcarrier $n \in \mathcal{N}_{\mathrm{a}}$
- T, MC-CDMA symbol period
- f_{c}, electronic carrier (passband) frequency
- $p(t)$, transmit pulse shape
- B, fixed bias of nonnegative passband signal for IM
- $A_{\max}$, maximum amplitude of QPSK symbol
- $s_{\mathrm{b}}(t)$, baseband MC-CDMA signal
- $s_{\mathrm{p}}(t)$, passband MC-CDMA signal
- $s_{\mathrm{opt}}(t)$, transmit optical signal
- E_{s}, QPSK symbol energy
- H_n, FFT of the discrete-time channel impulse response with length N symbol periods ($n \in \{0, \ldots, N-1\}$)

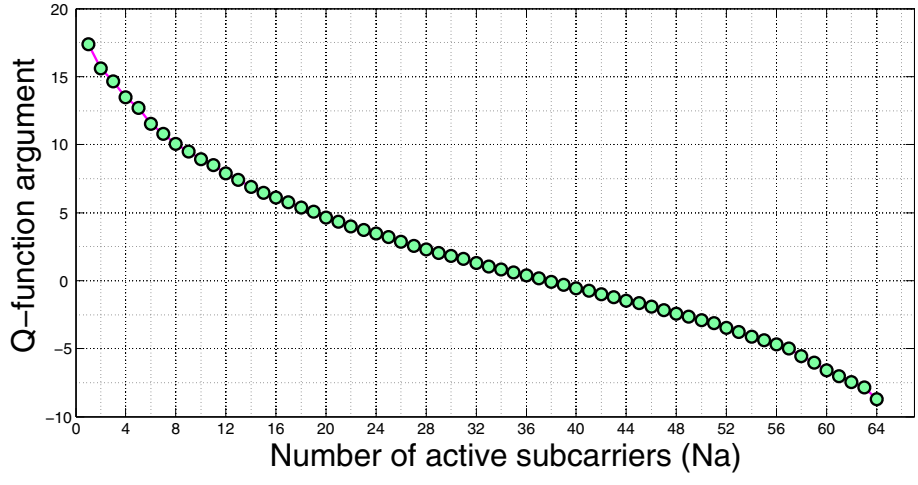

Figure 4 Q function argument vs. number of active subcarriers for the optical wireless domain.

Table 2 Q function arguments for both domains employing post-equalization-based subcarrier selection

Radio domain	Optical wireless domain
$\frac{N_a}{\sigma}\sqrt{\frac{E_s}{\left(\sum_{n\in\mathcal{N}_a} 1/\lvert H_n\rvert^2\right)}}$	$\frac{B_{post}}{L\sigma}\sqrt{\frac{T}{1+\gamma}}\sqrt{\frac{1}{\left(\sum_{n\in\mathcal{N}_a} 1/\lvert H_n\rvert^2\right)}}$

- W_n, complex AWGN values, which are iid circularly symmetric complex Gaussian rv with variance σ^2 (the variance of a complex random variable is the sum of the variance of the real part and that of the imaginary part).

Each user's binary data from the source is mapped onto complex-valued symbols d_l and spread in the frequency domain using a user-specific Walsh-Hadamard spreading code. Each CDMA codeword is assumed to be bipolar with its components belonging to the set $\{1, -1\}$. However, for convenience, we assume that a codeword component is equal to 0 on each inactive subcarrier. For example, out of eight subcarriers, if the first two and the last two subcarriers are active for user 0 and if the CDMA codeword for user 0 is $(1, -1, 1, -1)$, then we write

$$(c_0^0, c_1^0, c_2^0, c_3^0, c_4^0, c_5^0, c_6^0, c_7^0) = (1, -1, 0, 0, 0, 0, 1, -1).$$

Hence, users are distinguished by their respective code sequences. Every chip of the spreading code representing a fraction of the information symbol is transmitted through an active subcarrier. As described in Section 3.1, these active subcarriers are selected based on the CSI.

Figure 1 illustrates the transmission system model. An IFFT block modulates all QPSK data symbols corresponding to the total number of subcarriers. A cyclic prefix is inserted between each pair of successive symbols after converting them into a serial stream. Finally, the data signal is converted from digital to analog after which a fixed DC bias B is added to the signal to facilitate intensity modulation. When this signal travels through the medium, different subcarriers suffer different degradation and lose their mutual orthogonality. At the receiver, the DC bias is removed. After demodulation, each cyclic prefix is removed to obtain N-subcarrier components. The $N - N_a$ components are discarded after FFT and the remaining N_a components are despreaded to get each respective user-specific data symbol.

The above model is used to derive upper bounds for a fixed DC bias by employing pre-equalization and post-equalization schemes. For each case under investigation, CSI is assumed to be available at the transmitter or at the receiver as per post- or pre-equalization requirements, respectively. Then these fixed biases, denoted by B_{post} and B_{pre}, are employed in finding the optimal criteria for subcarrier selection in both cases. The following two subsections show the analytical models for both cases along with the derivation of conservative bounds for fixed DC biases. In both cases, subcarrier selection is based on maximizing the argument of the Q function in the BER expression, where the Q function is the complementary cumulative distribution function of zero-mean unit-variance Gaussian random variable.

3.2.1 Post-equalization case

At the transmitter, regardless of the number of active subcarriers N_a, the number of distinct symbols to be transmitted will always be N. The data symbols after the IFFT operation are represented as

$$D_k = \frac{1}{\sqrt{N}} \sum_{l=0}^{L-1} \sum_{n=0}^{N-1} d_l \cdot c_{l,n} e^{j2\pi kn/N}, k \in \{0, \ldots, N-1\}. \tag{3}$$

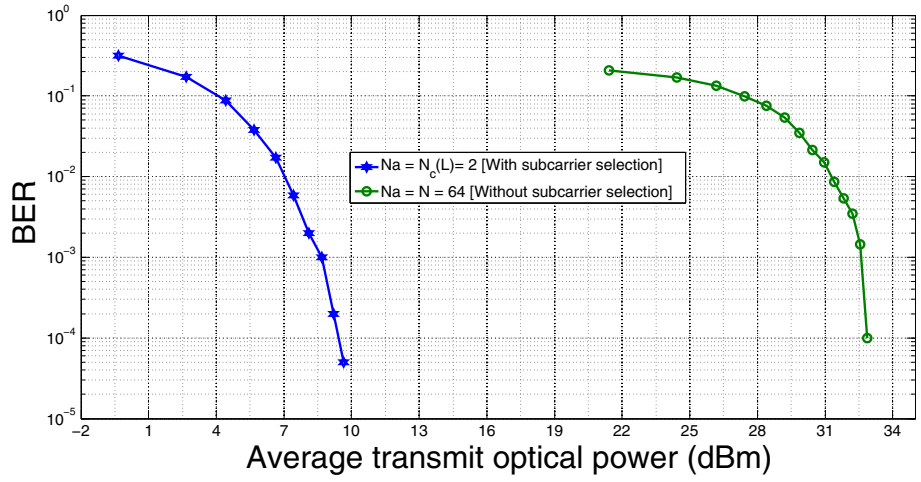

Figure 5 BER vs. transmit power with and without post-equalization-based subcarrier selection with two users.

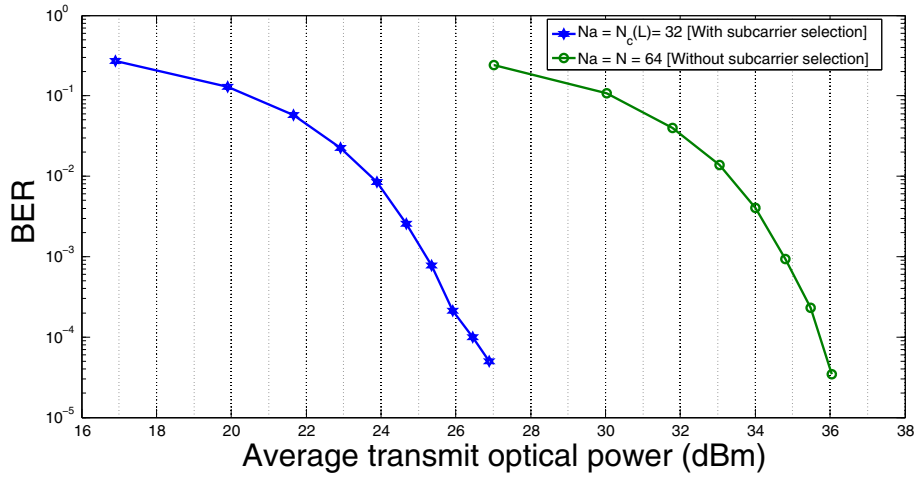

Figure 6 BER vs. transmit power with and without post-equalization-based subcarrier selection with 32 users.

The complex baseband transmitted signal is

$$s_{\mathrm{b}}(t) = \sum_{k=0}^{N-1} D_k p(t - kT/(1+\gamma)N) \tag{4}$$

where $p(t)$ is the unit norm rectangular transmit pulse shape of width $T/(1+\gamma)N$

$$p(t) = \begin{cases} \sqrt{\frac{(1+\gamma)N}{T}} & t \in (0, T/((1+\gamma)N)] \\ 0, & \text{otherwise.} \end{cases} \tag{5}$$

Hence, the real passband MC-CDMA signal to be used for IM is

$$s(t) = \mathrm{Re}\left[e^{j2\pi f_c t} \sum_{k=0}^{N-1} D_k p(t - kt/(1+\gamma)N) \right], \tag{6}$$

while the transmitted optical signal will be

$$s_{\mathrm{opt}}(t) = s(t) + B_{\mathrm{post}}. \tag{7}$$

We focus on the transmission period of the kth pulse, i.e., $p(t - kT/(1+\gamma)N)$. The real signal amplitude from (5) and (6) is given by

$$s(t) = \sqrt{\frac{(1+\gamma)N}{T}} \mathrm{Re}\left\{ D_k e^{j2\pi f_c t} \right\},$$
$$t \in \left[k\frac{T}{(1+\gamma)N}, (k+1)\frac{T}{(1+\gamma)N} \right].$$

For $f_c >> (1+\gamma)N/T$ (i.e., several periods of carrier waveform during the pulse interval), which is

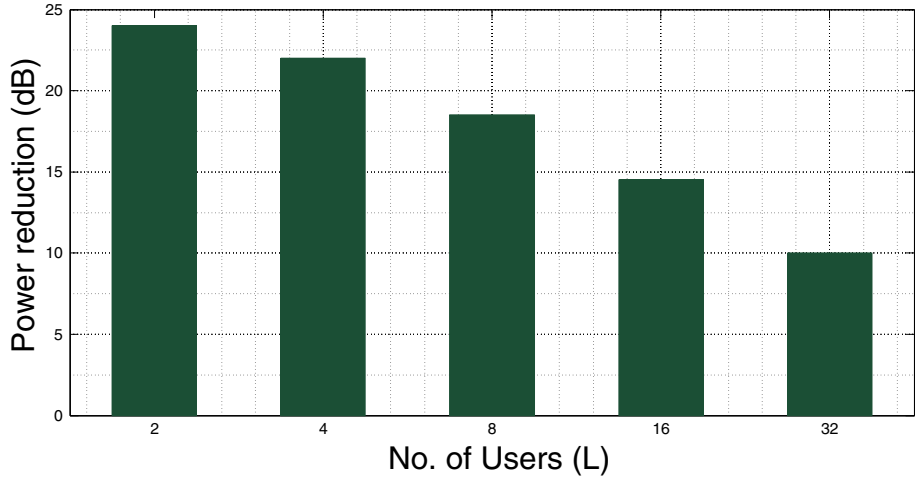

Figure 7 Power reduction for 2, 4, 8, 16, and 32 active users using post-equalization-based subcarrier selection.

typically the case, the minimum amplitude of $s(t)$ in $\left[k\frac{T}{(1+\gamma)N}, (k+1)\frac{T}{(1+\gamma)N}\right]$ can be taken as

$$-\sqrt{\frac{(1+\gamma)N}{T}}\left|D_k e^{j2\pi f_c t}\right| = -\sqrt{\frac{(1+\gamma)N}{T}}\,|D_k|\,.$$

It follows that the required bias during this interval is $\sqrt{\frac{(1+\gamma)N}{T}}|D_k|$, which can be bounded as

$$\begin{aligned} B_{\text{post}} &= \sqrt{\frac{(1+\gamma)N}{T}}|D_k| \\ &= \sqrt{\frac{(1+\gamma)N}{T}}\left|\frac{1}{\sqrt{N}}\sum_{l=0}^{L-1}\sum_{n=0}^{N-1} d_l \cdot c_{l,n}e^{j2\pi kn/N}\right| \\ &= \sqrt{\frac{1+\gamma}{T}}\left|\sum_{l=0}^{L-1}\sum_{n=0}^{N-1} d_l \cdot c_{l,n}e^{j2\pi kn/N}\right| \\ &\le \sqrt{\frac{1+\gamma}{T}}\sum_{l=0}^{L-1}\left|d_l\sum_{n=0}^{N-1} c_{l,n}e^{j2\pi kn/N}\right| \\ &\le \sqrt{\frac{1+\gamma}{T}}\sum_{l=0}^{L-1}|d_l|\left|\sum_{n=0}^{N-1} c_{l,n}e^{j2\pi kn/N}\right|. \end{aligned} \tag{8}$$

We are interested in the maximum negative value of the signal. Hence, we set $|d_l| \le A_{\max}$, which, in turn, depends upon the constellation configuration and the allocated subcarrier powers. Moreover, we set $C_{l,k} = \sum_{n=0}^{N-1} c_{l,n}e^{j2\pi kn/N}$. So inequality (8) becomes

$$B_{\text{post}} \le \sqrt{\frac{1+\gamma}{T}}A_{\max}\sum_{l=0}^{L-1} C_{l,k}.$$

To give an upper bound that is independent of k, i.e., fixed bias, the final expression is

$$B_{\text{post}} \le \max_{k\in\{0,1,\ldots,N-1\}}\sqrt{\frac{1+\gamma}{T}}A_{\max}\sum_{l=0}^{L-1} C_{l,k}. \tag{9}$$

Since only the data on the active subcarriers will be processed at the receiver

$$\begin{aligned} C_{l,k} &= \left|\sum_{n\in\mathcal{N}_a} c_{l,n}e^{j2\pi kn/N}\right| \\ &\le \sum_{n\in\mathcal{N}_a}\left|c_{l,n}e^{j2\pi kn/N}\right| = N_a, \end{aligned} \tag{10}$$

yielding an upper bound

$$\sum_{l=0}^{L-1} C_{l,k} \le LN_a. \tag{11}$$

The expression in (10) imposes an upper bound on the value of $C_{l,k}$, thus yielding a conservative value of the DC bias. Thus, from (9) and (11), we get

$$B_{\text{post}} \le \sqrt{\frac{1+\gamma}{T}}A_{\max}LN_a. \tag{12}$$

For the BER analysis, we shall focus on the equivalent baseband complex discrete-time system model. The received signals at the OFDM receiver can be expressed as vector $\mathbf{r} = (r_0, \ldots, r_{N-1})$ such that

$$r_n = H_n s_n + W_n, \tag{13}$$

where $(H_0, \ldots, H_{N-1})$ is the FFT of the discrete-time channel impulse response (whose length is N symbol periods), and W_ns are complex AWGN values. In particular, we assume that W_ns are iid circularly symmetric Gaussian random variables with variance σ^2 (when the noise PSD is given by $N_0/2$, we have $\sigma^2 = N_0/N$). For

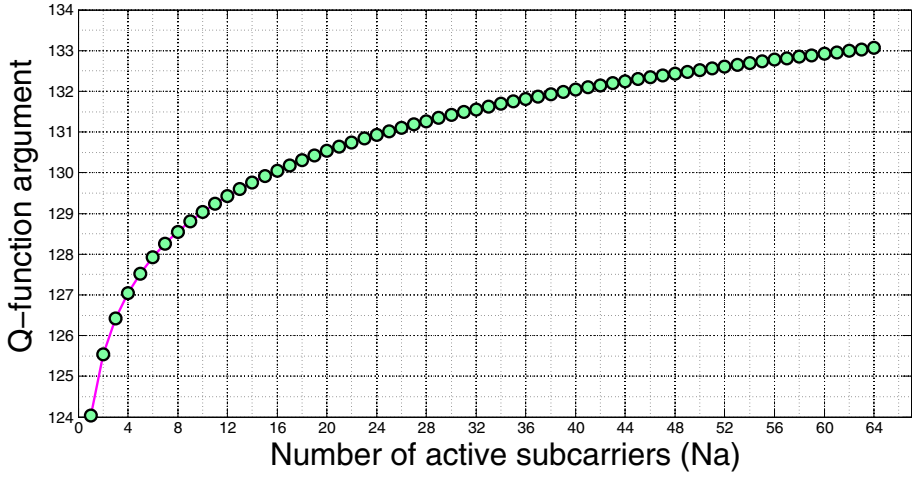

Figure 8 Q function argument vs. number of active subcarriers for the radio domain.

equalization as well as restoring the CDMA code orthogonality, we apply one-tap equalization to obtain $\mathbf{r}' = \left(r'_0, \ldots, r'_{N-1}\right)$ such that

$$r'_n = s_n + W_n/H_n. \tag{14}$$

From the equalized received signals, the QPSK symbol d_l can be obtained using the codeword $\mathbf{c}_l$, i.e., despreading. Let $\hat{d}_l$ be the received signal after despreading. In particular,

$$\hat{d}_l = \mathbf{c}_l^{\mathsf{T}}\mathbf{r}' = N_{\mathrm{a}} d_l + \sum_{n=1}^{N} c_{l,n} W_n/H_n. \tag{15}$$

For analyzing a user-specific performance, without loss of generality, we consider the received signal of user 0 ($\hat{d}_0$).

$$\hat{d}_0 = N_{\mathrm{a}} d_0 + \sum_{n=1}^{N} c_{0,n} W_n/H_n. \tag{16}$$

For QPSK, the BER can be found from the received symbol energy and the noise variance as

$$\begin{aligned}
\text{Received symbol energy} &= N_{\mathrm{a}}^2 E_{\mathrm{s}} \\
\text{Noise variance} &= \sigma^2 \left(\sum_{n \in \mathcal{N}_{\mathrm{a}}} 1/\left|H_n\right|^2 \right) \\
\mathrm{BER}_{\text{post-eq}} &= \mathcal{Q}\left(\frac{N_{\mathrm{a}}}{\sigma} \sqrt{\frac{E_{\mathrm{s}}}{\left(\sum_{n \in \mathcal{N}_{\mathrm{a}}} 1/\left|H_n\right|^2 \right)}} \right).
\end{aligned} \tag{17}$$

For QPSK, using $A_{\max} = \sqrt{E_{\mathrm{s}}}$ in (12), the BER in terms of the DC bias is found to be

$$\mathrm{BER}_{\text{post-eq}} = \mathcal{Q}\left(\frac{B_{\text{post}}}{L\sigma} \sqrt{\frac{T}{1+\gamma}} \sqrt{\frac{1}{\sum_{n \in \mathcal{N}_{\mathrm{a}}} 1/\left|H_n\right|^2}} \right) \tag{18}$$

Subcarrier selection: post-equalization case. The BER expression in (18) yields the following theorem that provides a method to select active subcarriers. Let $N_{\mathrm{c}}(L)$ denote the length of CDMA codewords required to accommodate L users. Note that the value $N_{\mathrm{c}}(L)$ depends on the type of codewords used.

Theorem 1. *Given that we use the DC bias in (12), the set of active subcarriers that yields the minimum BER is selected as follows:*

1. *The number of active subcarriers is $N_{\mathrm{c}}(L)$.*
2. *The selected active subcarriers are the $N_{\mathrm{c}}(L)$ subcarriers with the highest gain magnitudes, i.e., highest $|H_n|$s.*

Proof. Minimize the BER expression in (18) over $N_{\mathrm{c}}(L) \le N_{\mathrm{a}} \le N$ is equivalent to solving the following optimization problem:

$$\begin{aligned}
\text{maximize} \quad & \xi = \sqrt{\frac{1}{\sum_{n \in \mathcal{N}_{\mathrm{a}}} 1/\left|H_n\right|^2}} \\
\text{subject to} \quad & N_{\mathrm{c}}(L) \le N_{\mathrm{a}} \le N
\end{aligned}$$

The value of ξ is decreasing with N_{a} since $|H_n|$'s are always positive. Consequently, the smallest possible value of N_{a} is optimal. Since we need to use at least $N_{\mathrm{c}}(L)$ subcarriers, it follows that $N_{\mathrm{a}} = N_{\mathrm{c}}(L)$. This proves part 1.

Now, given that we must use $N_{\mathrm{c}}(L)$ subcarriers, the best choice is to select the subcarriers with the highest magnitude gains to maximize ξ. This proves part 2. □

3.2.2 Pre-equalization case

When equalization is employed at the transmitter, every data symbol is weighted by $1/H_n$. Accordingly, the data symbols after the IFFT operation are represented as

$$D_k = \frac{1}{\sqrt{N}} \sum_{l=0}^{L-1} \sum_{n=0}^{N-1} \frac{d_l \cdot c_{l,n}}{H_n} e^{j2\pi kn/N}. \tag{19}$$

After a similar treatment as in the case of post-equalization, we get the fixed DC bias B_{pre} as follows

$$\begin{aligned}
B_{\text{pre}} &= \sqrt{\frac{(1+\gamma)N}{T}} \left|D_k\right| \qquad (20) \\
&= \sqrt{\frac{(1+\gamma)N}{T}} \left| \frac{1}{\sqrt{N}} \sum_{l=0}^{L-1} \sum_{n=0}^{N-1} \frac{d_l \cdot c_{l,n}}{H_n} e^{j2\pi kn/N} \right| \\
&= \sqrt{\frac{1+\gamma}{T}} \left| \sum_{l=0}^{L-1} \sum_{n=0}^{N-1} \frac{d_l \cdot c_{l,n}}{H_n} e^{j2\pi kn/N} \right| \\
&\le \sqrt{\frac{1+\gamma}{T}} \sum_{l=0}^{L-1} \left| d_l \sum_{n=0}^{N-1} \frac{c_{l,n}}{H_n} e^{j2\pi kn/N} \right| \\
&\le \sqrt{\frac{1+\gamma}{T}} \sum_{l=0}^{L-1} \left|d_l\right| \left| \sum_{n=0}^{N-1} \frac{c_{l,n}}{H_n} e^{j2\pi kn/N} \right|. \qquad (21)
\end{aligned}$$

We are interested in the maximum negative value of the signal. Hence, we set $|d_l| \le A_{\max}$, which, in turn, depends upon the constellation configuration and the allocated subcarrier power. Moreover, we set $C'_{l,k} = \left| \sum_{n=0}^{N-1} \frac{c_{l,n}}{H_n} e^{j2\pi kn/N} \right|$. So inequality (21) becomes

$$B_{\text{pre}} \le \sqrt{\frac{1+\gamma}{T}} A_{\max} \sum_{l=0}^{L-1} C'_{l,k}.$$

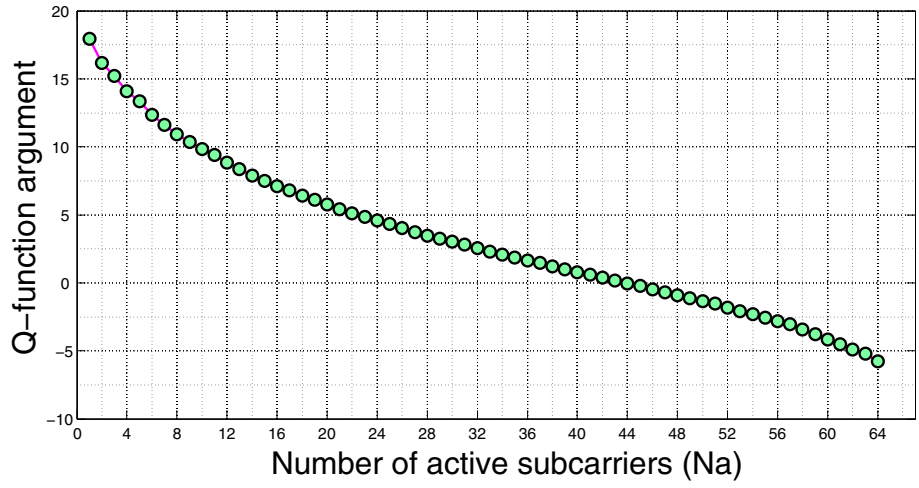

Figure 9 Q function argument vs. number of active subcarriers for the optical wireless domain.

To give an upper bound that is independent of k, i.e., fixed bias, the final expression is

$$B_{\text{pre}} \leq \max_{k\in\{0,1,\ldots,N-1\}} \sqrt{\frac{1+\gamma}{T}} A_{\max} \sum_{l=0}^{L-1} C'_{l,k}. \tag{22}$$

Since only the data on the active subcarriers will be processed at the receiver, we can generalize in a similar fashion as in the case of post-equalization,

$$\begin{aligned} C'_{l,k} &= \left| \sum_{n\in\mathcal{N}_{\text{a}}} \frac{c_{l,n}}{H_n} e^{j2\pi kn/N} \right| \\ &\leq \sum_{n\in\mathcal{N}_{\text{a}}} \left| \frac{c_{l,n}}{H_n} e^{j2\pi kn/N} \right| = \sum_{n\in\mathcal{N}_{\text{a}}} \frac{1}{|H_n|}, \end{aligned} \tag{23}$$

yielding an upper bound

$$\sum_{l=0}^{L-1} C'_{l,k} \leq L \sum_{n\in\mathcal{N}_{\text{a}}} \frac{1}{|H_n|}. \tag{24}$$

The expression in (23) imposes an upper bound on the value of $C'_{l,k}$, thus yielding a conservative value of the DC bias. Thus, from (22) and (24), we get

$$B_{\text{pre}} \leq \sqrt{\frac{1+\gamma}{T}} A_{\max} L \sum_{n\in\mathcal{N}_{\text{a}}} \frac{1}{|H_n|}. \tag{25}$$

By proceeding in the similar fashion as in the case of post-equalization and incorporating noise variance $= \sigma^2 N_{\text{a}}$, we get the BER expression as

$$\text{BER}_{\text{pre-eq}} = \mathcal{Q}\left(\frac{1}{\sigma} \sqrt{E_s N_{\text{a}}} \right). \tag{26}$$

Using (25) and incorporating $A_{\max} = \sqrt{E_{\text{s}}}$ for QPSK, the BER expressing in terms of the DC bias is

$$\text{BER}_{\text{pre-eq}} = Q\left(\sqrt{\frac{TN_{\text{a}}}{1+\gamma}} \frac{B_{\text{pre}}}{L\sigma \sum\limits_{n\in\mathcal{N}_{\text{a}}} 1/|H_n|} \right). \tag{27}$$

Subcarrier selection: pre-equalization case. The BER expression in (27) yields the following theorem that provides a method to select active subcarriers.

Theorem 2. *Given that we use the DC bias in (25), the set of active subcarriers that yields the minimum BER is selected as follows:*

1. *The number of active subcarriers is $N_{\text{c}}(L)$.*
2. *The selected active subcarriers are the $N_{\text{c}}(L)$ subcarriers with the highest gain magnitudes i.e., highest $|H_n|$s.*

Proof. Minimizing the BER expression in (27) over $N_{\text{c}}(L) \leq N_{\text{a}} \leq N$ is equivalent to solving the following optimization problem:

$$\begin{aligned} \text{maximize} \quad & \kappa = \frac{\sqrt{N_{\text{a}}}}{\sum\limits_{n\in\mathcal{N}_{\text{a}}} 1/|H_n|} \\ \text{subject to} \quad & N_{\text{c}}(L) \leq N_{\text{a}} \leq N \end{aligned}$$

Table 3 Q function arguments for both domains employing pre-equalization-based subcarrier selection

Radio domain	Optical wireless domain
$\frac{1}{\sigma}\sqrt{E_S N_{\text{a}}}$	$\sqrt{\frac{TN_{\text{a}}}{1+\gamma}} \frac{B_{\text{pre}}}{L\sigma \sum\limits_{n\in\mathcal{N}_{\text{a}}} 1/\lvert H_n\rvert}$

Since $|H_n|$s are smaller than 1 (i.e., signal attenuation typically in the order of 10^{-7}), κ decreases with N_a. Consequently, the smallest possible value of N_a is optimal. Since we need to use at least $N_c(L)$ subcarriers, it follows that $N_a = N_c(L)$. This proves part 1.

Now, given that we must use $N_c(L)$ subcarriers, the best choice is to select the subcarriers with the highest magnitude gains to maximize κ. This proves part 2. □

3.3 Comparison between $\mathrm{BER}_{\text{post-eq}}$ and $\mathrm{BER}_{\text{pre-eq}}$

From the previous discussions, we conclude that for both post-equalization and pre-equalization it is optimal to select $N_c(L)$ subcarriers with the highest $|H_n|$s. The next question is whether post-equalization or pre-equalization performs better in terms of the BER for a given DC bias $B_{\text{post}} = B_{\text{pre}} = B$.

The next theorem shows that pre-equalization always performs no worse than post-equalization.

Theorem 3. *Given that the DC biases in (12) and (25) are used for post-equalization and pre-equalization respectively, the corresponding BER for pre-equalization is no more than the BER for post-equalization.*

Proof. We first rewrite the post-equalization BER expression of (18) as

$$\mathrm{BER}_{\text{post-eq}} = \mathcal{Q}\left(\frac{B}{L\sigma}\sqrt{\frac{T}{(1+\gamma)N_a}}\sqrt{\frac{N_a}{\sum\limits_{n\in\mathcal{N}_a} 1/|H_n|^2}}\right). \tag{28}$$

We proceed in a similar fashion from the pre-equalization BER expression of (27) to obtain

$$\mathrm{BER}_{\text{pre-eq}} = \mathcal{Q}\left(\frac{B}{L\sigma}\sqrt{\frac{T}{(1+\gamma)N_a}}\frac{N_a}{\sum\limits_{n\in\mathcal{N}_a} 1/|H_n|}\right). \tag{29}$$

In (28) and (29), the first two factors in the arguments of the Q function are identical (denoted by α). Hence,

$$(28) \implies \mathrm{BER}_{\text{post-eq}} = \mathcal{Q}\left(\alpha\sqrt{\frac{N_a}{\sum\limits_{n\in\mathcal{N}_a} 1/|H_n|^2}}\right)$$

$$\text{and}(29) \implies \mathrm{BER}_{\text{pre-eq}} = \mathcal{Q}\left(\alpha\frac{N_a}{\sum\limits_{n\in\mathcal{N}_a} 1/|H_n|}\right).$$

From the direct consequence of the Cauchy-Schwarz inequality $\frac{\sum_{i=0}^{n} x_i}{n} \le \sqrt{\frac{\sum_{i=0}^{n} x_i^2}{n}}$, the inequality $\frac{N_a}{\sum_{n\in\mathcal{N}_a} 1/|H_n|} \ge \sqrt{\frac{N_a}{\sum_{n\in\mathcal{N}_a} 1/|H_n|^2}}$ holds. It follows that $\mathrm{BER}_{\text{pre-eq}} \le \mathrm{BER}_{\text{post-eq}}$. □

4 Analytical and simulation results with discussions

Based on the system model of MC-CDMA-based indoor optical wireless communications and the simulation parameters shown in Table 1, the system is simulated using MATLAB for observing power reduction performance using optimal number of subcarriers (from Theorem 1 and 2 developed in Section 3) with respect to using all available subcarriers.

For 10-Mbps 64-subcarrier system, the subcarriers' channel gains are shown in Figure 2. The observed variations in the channel gains can be exploited for subcarrier selection at high data rates of the same order. Besides improving the BER performance of the system, this fact is used to reduce the DC bias and hence average transmit optical power, as will be demonstrated in the subsequent graphs.

4.1 Post-equalization-based subcarrier selection

Figures 3 and 4 show the analytical curves for the argument of the Q function for 10 Mbps in the case of the radio domain and the optical wireless domain, respectively, when employing successively an increasing number of active subcarriers (with decreasing channel gain magnitudes) in an MC-CDMA-based indoor optical wireless IM/DD system with 64 subcarriers. The expressions for the Q function arguments (derived in Section 3.2.1) for both domains are shown in Table 2.

It can be observed in Figure 3 that an optimal number of active subcarriers exists in the range $1 < N_a < N$ for the radio domain. The behavior is different for the optical wireless domain where it is always better to have fewer active subcarriers, as can be observed in Figure 4. This reveals the fact that there is a fundamental difference in subcarrier selection between radio communications and optical wireless communications employing post-equalization. The optimal number of subcarriers to be employed is consistent with Theorem 1 of Section 3.2.1.

Considering the case of using all available subcarriers as the baseline, investigation is made for average transmit optical power reduction subject to a BER requirement of 10^{-4}. The baseline of 10^{-4} is used because we focus on uncoded transmissions. With error control coding, which is typically used in practical systems, the BER can be driven down by few order of magnitudes [31,32]. Figures 5 and 6 show the simulation curves depicting BER performance and power reduction for the considered

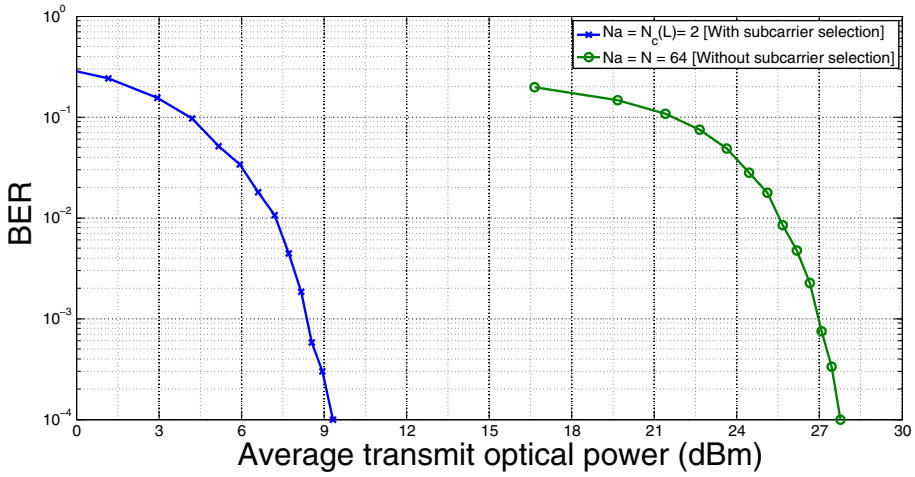

Figure 10 BER vs. transmit power with and without pre-equalization-based subcarrier selection two users.

system with and without subcarrier selection based on post-equalization at the receiver for 2 and 32 users, respectively. The values of 2 and 32 users are considered to check the average transmit power for extreme cases. Subcarrier selection in Theorem 1 is employed to choose out of the total of 64 subcarriers. A reduction of about 24 dB for 2 users and about 10 dB for 32 users can be observed from the graph for a BER requirement of 10^{-4}.

Transmit optical power reduction for $L = 2, 4, 8, 16, 32$ active users using optimal number of subcarriers based on Theorem 1 is next investigated. Simulation results for the system under consideration, i.e., with 64 subcarriers and 10-Mbps data transmission rate, are shown in Figure 7. Each bar in the graph depicts the magnitude of average transmit optical power reduction. It is evident from the figure that although the power reduction magnitude decreases as the number of users increases, this reduction is significant for up to a moderate number of users (wrt total number of subcarriers).

4.2 Pre-equalization-based subcarrier selection

Figures 8 and 9 show the analytical curves for the argument of the Q function for 10-Mbps in case of the radio domain and the optical wireless domain, respectively, when employing successively an increasing number of active subcarriers (with decreasing channel gain magnitudes) in an MC-CDMA-based indoor optical wireless IM/DD system with 64 subcarriers. These curves exhibit different behaviors from those of post-equalization-based subcarrier selection. The expressions for the Q function arguments (derived in Section 3.2.2) for both domains are shown in Table 3.

Based on Figure 8, in radio communications employing subcarrier selection based on pre-equalization, a lower

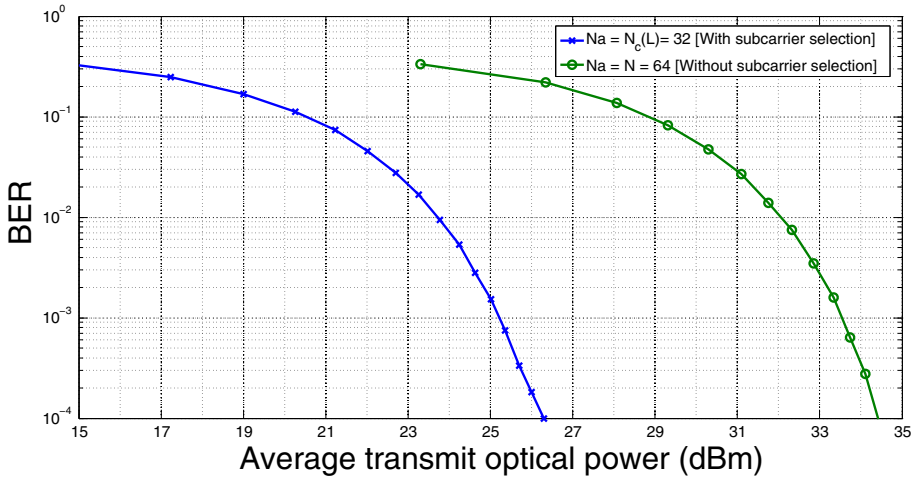

Figure 11 BER vs. transmit power with and without pre-equalization-based subcarrier selection with 32 users.

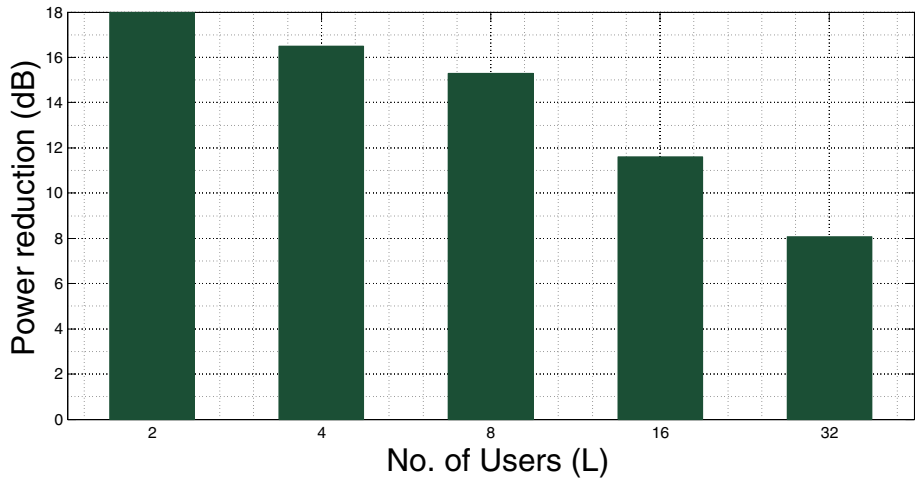

Figure 12 Power reduction for 2, 4, 8, 16, and 32 active users using pre-equalization-based subcarrier selection.

BER is obtained by employing more subcarriers for data transmission. The case is exactly opposite for optical wireless communications, as can be observed in Figure 9, where a lower BER results from using fewer active subcarriers. This reveals the fact that there is a fundamental difference in subcarrier selection between radio communications and optical wireless communications employing pre-equalization. The optimal number of subcarriers to be employed is consistent with Theorem 2 of Section 3.2.2.

Considering the case of using all available subcarriers as the baseline, investigation is made for average transmit optical power reduction subject to a BER requirement of 10^{-4}. Figures 10 and 11 show the simulation curves depicting BER performance and power reduction for the mentioned system with and without subcarrier selection based on pre-equalization at the transmitter for 2 and 32 users respectively. A reduction of 18 dB for 2 users and 8 dB for 32 users can be observed from the graphs for a BER requirement of 10^{-4}.

Similar to the case of post-equalization-based subcarrier selection, investigation is carried out to identify power reduction for $L = 2, 4, 8, 16, 32$ MC-CDMA users for pre-equalization-based subcarrier selection according to Theorem 2. It is clear from Figure 12 that the optical transmit power reduction decreases with the number of users. However, this reduction is significant for up to a moderate number of users.

5 Conclusions

We proposed and investigated pre- and post-equalization-based subcarrier selection approaches as efficient modes of average transmit optical power reduction in an MC-CDMA-based indoor optical wireless communication system with IM/DD. Based on these approaches, conservative expressions for fixed DC biases to be employed in the system are derived. We then used the established DC bias expressions to construct optimal methods for choosing the number of active subcarriers for both pre- and post-equalization.

The simulation results validate the correctness of analytically found optimal criteria of subcarrier selection. For up to a moderate number of users, as is the case in indoor optical wireless communication systems, the amount of transmit power reduction can be significant. A typical data transmission rate of 10 Mbps with 64 subcarriers and QPSK modulation is used as an example case. For post-equalization-based subcarrier selection, reductions ranging from 10 to 24 dB are observed while 8 to 18 dB are observed for pre-equalization-based subcarrier selection with the BER requirement of 10^{-4}. Finally, analytical comparison of both cases reveals that pre-equalization always performs no worse than post-equalization in terms of the BER for the same optical transmit power.

Competing interests
Both authors declare that they have no competing interests.

Acknowledgments
The authors would like to pay gratitude to the Higher Education Commission (HEC), Pakistan, for supporting this research work and for the continuous encouragement in higher education.

Received: 12 June 2012 Accepted: 13 May 2013
Published: 28 May 2013

References

1. A Paraskevopoulos, J Vucic, SH Voss, R Swoboda, KD Langer, Optical wireless communication systems in the Mb/s to Gb/s range, suitable for industrial applications. IEEE/ASME Trans. Mechatronics. **15**, 541–547 (2010)
2. K Wang, A Nirmalathas, C Lim, E Skafidas, High-speed optical wireless communication system for indoor applications. IEEE Photonics Tech. Lett. **23**, 519–521 (2011)

3. R You, JM Kahn, Average power reduction techniques for multiple-subcarrier intensity-modulated optical signals. IEEE Trans. Commun. **49**, 2164–2171 (2001)
4. H Joshi, RJ Green, MS Leeson, in *10th Anniversary Proceedings of the IEEE International Conference on Transparent Optical Networks*. Multiple sub-carrier optical wireless systems. Athens, 22–26 June 2008
5. S Hranilovic, *Wireless Optical Communication Systems*, 1st edn. (Springer, Boston, 2005)
6. L Chen, B Krongold, J Evans, in *IEEE International Conference on Communications ICC*. Performance evaluation of optical OFDM systems with nonlinear clipping distortions. Dresden, 14–18 June 2009
7. J Armstrong, AJ Lawery, Power efficient optical OFDM. IEEE Electron. Lett. **42**, 370–372 (2006)
8. JM Kahn, JR Barry, Wireless infrared communications. Proc. IEEE. **85**, 265–298 (1997)
9. JB Carruthers, in *Wiley Encyclopedia of Telecommunications*. 2nd edn., vol. 2, ed. by JG Proakis. Wireless infrared communications (Wiley, New York, 2003), pp. 53–76
10. M Sharif, B Hassibi, On the achievable average power reduction of MSM optical signals. IEEE Commun. Lett. **8**, 84–86 (2004)
11. R Mesleh, H Elgala, H Haas, in *Proceedings of the 7th International Symposium on Communication Systems Network and Digital Signal Processing - CSNDSP'10*. An overview of indoor OFDM/DMT optical wireless communication systems. Newcastle, 21–23 July 2010
12. W Kang, S Hranilovic, in *Proceedings of the 23rd Biennial Symposium on Communications*. In-band coding for power reduction in multiple-subcarrier modulated wireless optical systems. Kingston, 29 May–1 June 2006, pp. 96–99
13. W Kang, S Hranilovic, Power reduction techniques for multiple-subcarrier modulated diffuse wireless optical channels. IEEE Trans. Commun. **56**, 279–288 (2008)
14. MZ Farooqui, P Saengudomlert, S Kaiser, in *Proceedings of the International Conference on Electrical and Computer Engineering, ICECE'10*. Average transmit power reduction in OFDM-based indoor wireless optical communications using SLM. Dhaka, 18–20 December 2010
15. MZ Farooqui, P Saengudomlert, in *Proceedings of the 8th Electrical Engineering/Electronics, Computer, Telecommunications and Information Technology Association of Thailand Conference, ECTI-CON'11*. Average transmit power reduction through power allocation for OFDM-based indoor wireless optical communications. Khon Kaen, 17–19 May 2011
16. J Ilic, T Strohmer, Average power reduction for MSM optical signals via sparsity and uncertainty principle. IEEE Trans. Commun. **58**, 1505–1513 (2010)
17. MS Moreolo, R Munoz, G Junyent, Novel power efficient optical OFDM based on Hartley transform for intensity-modulated direct-detection systems. J. Lightwave Tech. **28**, 798–805 (2010)
18. J Grubor, KD Langer, Efficient signal processing in OFDM-based indoor optical wireless links. J. Netw. **5**, 197–211 (2010)
19. R You, JM Kahn, Upper-bounding the capacity of optical IM/DD channels with multiple-subcarrier modulation and fixed bias using trigonometric moment space method. IEEE Trans. Inf. Theory. **48**, 514–523 (2002)
20. K Fazel, S Kaiser, *Multi-Carrier and Spread Spectrum Systems*. (Wiley, West Sussex, 2003)
21. BM Masini, F Zabini, in *Proceedings of the IEEE Wireless Communications and Networking Conference, WCNC*. On the effect of combined equalization for MC-CDMA systems in correlated fading channels. Budapest, 5–8 April 2009
22. L Sanguinetti, I Cosovic, M Morelli, Channel estimation for MC-CDMA uplink transmissions with combined equalization. IEEE J. Selected Areas Commun. **24**, 1167–1178 (2006)
23. D Mottier, D Castelain, in *Proceedings of the Personal, Indoor, Mobile Radio Communications*. SINR-based channel pre-equalization for uplink multi-carrier CDMA systems. Lisboa, 15–18 September 2002
24. S Nobilet, JF Herald, in *Proceedings of the IEEE 56th Vehicular Technology Conference*, vol. 1. A pre-equalization technique for uplink MC-CDMA systems using TDD and FDD modes,Vancouver, BC, Canada (Picataway IEEE, 2002), pp. 346–350
25. N Benvenuto, P Bisaglia, F Tosato, Pre-equalization with subband channel loading: a technique to maximize throughput in uplink OFDM-CDMA systems. IEEE Trans. Commun. **53**, 564–568 (2005)
26. B Masini, F Zabini, A Conti, in *Communications and Networking*, ed. by J Peng. MC-CDMA systems: a general framework for performance evaluation with linear equalization (Rijeka, Croatia Sciyo, 2010), pp. 127–148
27. L Hanzo, LL Yang, EL Kuan, K Yen, *Single and Multi-Carrier DS-CDMA: Multi-User Detection, Space-Time Spreading, Synchronisation, Networking and Standards*. (Wiley-IEEE, West Sussex, 2003)
28. I Cosovic, L Sanguinetti, in *IEEE 61st Vehicular Technology Conference*. On the peak-to-average power ratio of pre-equalized multi-carrier code-division multiple-access transmissions. Stockholm, 30 May–1 June 2005
29. DK Borah, AC Boucouvalas, CC Davis, S Hranilovic, K Yiannopoulos, A review of communication-oriented optical wireless systems. EURASIP J. Wireless Commun. Netw. **91**, 1–28 (2012)
30. D O'Brien, HL Minh, G Faulkner, M Wolf, L Grobe, J Li, O Bouchet, in *IEEE Globecom Workshop on Optical Wireless Communications*. High data-rate infra-red optical wireless communications: implementation challenges. Miami,6–10 December 2010
31. G Ntogari, T Kamalakis, T Sphicopoulos, Performance analysis of space time block coding techniques for indoor optical wireless systems. IEEE. J. Selected Areas Commun. **27**(9), 1545–1552 (2009)
32. J Li, M Uysal, in *58th IEEE Vehicular Technology Conference*, vol. 1. Optical wireless communications: system model, capacity and coding (IEEE Piscataway, 2003)

doi:10.1186/1687-1499-2013-138
Cite this article as: Farooqui and Saengudomlert: **Transmit power reduction through subcarrier selection for MC-CDMA-based indoor optical wireless communications with IM/DD.** *EURASIP Journal on Wireless Communications and Networking* 2013 **2013**:138.